Accepted Manuscript

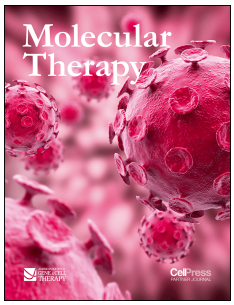

Long Terminal Repeat CRISPR-CAR coupled 'universal' T cells mediate potent anti-leukemic effects

Christos Georgiadis, Roland Preece, Lauren Nickolay, Aniekan Etuk, Anastasia Petrova, Dariusz Ladon, Alexandra Danyi, Neil Humphryes-Kirilov, Ayokunmi Ajetunmobi, Daesik Kim, Jin-Soo Kim, Waseem Qasim

PII: S1525-0016(18)30096-0

DOI: 10.1016/j.ymthe.2018.02.025

Reference: YMTHE 4587

To appear in: *Molecular Therapy*

Received Date: 10 November 2017

Accepted Date: 25 February 2018

Please cite this article as: Georgiadis C, Preece R, Nickolay L, Etuk A, Petrova A, Ladon D, Danyi A, Humphryes-Kirilov N, Ajetunmobi A, Kim D, Kim J-S, Qasim W, Long Terminal Repeat CRISPR-CAR coupled 'universal' T cells mediate potent anti-leukemic effects, *Molecular Therapy* (2018), doi: 10.1016/j.ymthe.2018.02.025.

Title:

Long Terminal Repeat CRISPR-CAR coupled 'universal' T cells mediate potent anti-leukemic effects

Christos Georgiadis[1*], Roland Preece[1*], Lauren Nickolay[1], Aniekan Etuk[1], Anastasia Petrova[1], Dariusz Ladon[2], Alexandra Danyi[3], Neil Humphryes-Kirilov[3], Ayokunmi Ajetunmobi[3], Daesik Kim[4], Jin-Soo Kim[4], Waseem Qasim[1,2]

[1]Molecular and Cellular Immunology Unit, UCL Great Ormond Street Institute of Child Health, London, WC1N 1EH

[2] NIHR Great Ormond Street Hospital Biomedical Research Centre, 30 Guilford Street, London WC1N 1EH

[3]Desktop Genetics Ltd, 28 Hanbury Street, London, E1 6QR

[4]Department of Chemistry, Seoul National University, Seoul, South Korea

*These authors contributed equally

Running title: Potent anti-leukemic effect of CRISPR-CAR T cells

Keywords: B-ALL, CAR T cells, CRISPR/Cas9 gene editing, lentiviral vector gene therapy

Word count: 4,848

Abstract word count: 201

Figure count: 5

Reference count: 36

Abstract

Gene editing can be used to overcome allo-recognition which otherwise limits allogeneic T cell therapies. Initial proof-of-concept applications have included generation of such 'universal' T cells expressing chimeric antigen receptors (CAR) against CD19 target antigens combined with transient expression of DNA-targeting nucleases to disrupt the T cell receptor alpha constant chain (TRAC). While relatively efficient, transgene expression and editing effects were unlinked, yields variable, and resulting T cell populations heterogeneous, complicating dosing strategies. We describe a self-inactivating lentiviral 'terminal' vector platform coupling CAR expression with CRISPR/Cas9 effects through incorporation of an sgRNA element into the ΔU3 3' long terminal repeat (LTR). Following reverse transcription and duplication of the hybrid ΔU3-sgRNA, delivery of Cas9 mRNA resulted in targeted TRAC locus cleavage and allowed the enrichment of highly homogenous (>96%) CAR+ (>99%) TCR- populations by automated magnetic separation. Molecular analyses, including NGS, WGS and Digenome-seq verified on-target specificity with no evidence of predicted off-target events. Robust anti-leukemic effects were demonstrated in humanized immunodeficient mice and were sustained longer than by conventional CAR+TCR+ T cells. Terminal-TRAC (TT) CAR T cells offer the possibility of a pre-manufactured, non-HLA matched CAR cell therapy and will be evaluated in phase 1 trials against B cell malignancies shortly.

Introduction

T cells engineered to express recombinant antigen specific receptors or chimeric antigen receptors are in multi-phase trials, with some approaches yielding compelling remission effects against refractory leukemia.[1] The majority of subjects treated to date have provided and received autologous T cells, but this approach may not be best suited for widespread cost-effective delivery of cellular therapy. Gene editing offers the prospect of addressing HLA- barriers and the development of universal T cell therapies.[2, 3] Recently T cells modified using transcription activator-like effector nucleases (TALENs) and expressing chimeric antigen receptor (CAR) against CD19 have been used to treat refractory relapsed B cell acute lymphoblastic leukemia (B-ALL) in infants.[4] These 'off-the-shelf' cells were derived from a non-HLA matched donor and were disrupted for CD52 expression to evade the depletion effects of Alemtuzumab, and were simultaneously modified at the T cell receptor (TCR) alpha chain constant (TRAC) region and depleted of T cells expressing TCRαβ to reduce the risk of graft versus host disease (GVHD).[5] Clinical trials are underway to assess the strategy further in children and adults, and key aspects determining dosing schedules related to carriage of residual TCRαβ T cells and proportion of cells expressing CAR19. The former comprise <1% of the total cell inoculum after TCRαβ magnetic bead depletion, but constitute a risk for GVHD and are strictly capped to below $5x10^4$ T cells/kg.[6] This in turn limits the total cell dose, and because only a proportion of cells express CAR19 as a result of batch-to-batch variation in lentiviral transduction efficiency, the total cell dosing regimen differs between batches. Similar issues arise for other gene editing platforms relying on segregated DNA nuclease delivery, whether by non-integrating viral delivery of Zinc Finger Nucleases [3] or megaTALs combined with non-viral delivery.[7]

We designed a self-inactivating (SIN)-lentiviral platform that coupled transgene expression with clustered regularly interspersed short palindromic repeats (CRISPR) editing effects for efficient and homogenous T cell modification (Figure 1A), and demonstrated that this system is scalable and can be incorporated into a largely automated manufacturing process. CRISPR mediated effects in CAR19 modified T cells have been reported previously. For example, Ren et al used CRISPR RNA electroporation to disrupt endogenous TCR and β_2-microglobulin (B_2m) genes for disruption of MHC class I in T cells transduced with a lentiviral CAR vector, but editing and transgene effects were unlinked.[8, 9] Other lentiviral configurations have incorporated both CRISPR guide sequences and Cas9 expression cassettes which become integrated into the target cell genome as a constituent of proviral vector DNA.[10] While suitable for pre-clinical studies, constitutive expression of Cas9 would be problematic in human trials, not least because of its bacterial origin and likely immunogenicity. In order to overcome this issue, we delivered capped, polyadenylated, uridine modified Cas9 mRNA by electroporation to T cells that had been transduced with our 'terminal-CRISPR' lentiviral configuration. Here, CAR19 was expressed under the control of an internal human promoter and CRISPR guide sequences and associated H1/U6 promoters were incorporated into the U3 region of the 3' long terminal repeat (LTR) sequence of the vector. Previous vector configurations using these flanking regions have included a γ-retroviral vector for expression of cDNA cassettes [11], and a lentiviral system encoding short hairpin RNA interference elements.[12] Modification of the LTR can impair retroviral titres, but has a number of advantages, including avoiding interference with internal promoters [13] and duplication of sequences cited in the U3 locus following reverse transcription. Here we adopt and refine this approach for CRISPR delivery, anticipating guide duplication and incorporation into the 5' LTR during reverse transcription and vectorized linkage of guide effects with transgene

expression. We demonstrate compliant scalability and the potential of the platform for the generation of ‘universal’ human T cells on a clinical scale. Potent anti-leukemic effects of TCR depleted CAR19 T cells were demonstrated in a human:murine chimeric tumor model. Multi-modal analysis confirmed highly efficient ‘on-target’ modifications with no predicted or unpredicted ‘off-target’ events recorded.

Results

Design and construction of lentiviral terminal-TRAC (TT) guide RNA vectors

Incorporation of a Pol III promoter and single-guide-RNA (sgRNA) sequence into the 3' LTR of a U3 deleted third generation lentiviral vector, generated a self-duplicating CRISPR expression cassette (Figure 1B). A region immediately proximal to 3' repeat (R) regions was selected to preserve reverse transcription mediated duplication to the 5' LTR, resulting in a proviral form with both 5' and 3' flanking terminal CRISPR elements (Figure 1C). For targeting of endogenous TCR expression, a sgRNA sequence targeting the TRAC locus (specificity score 94/100[14]) was placed under the control of the human Pol III promoter, U6, followed by a sgRNA sequence specific for *S.pyogenes* Cas9, which was delivered separately as mRNA by electroporation (Figure 1D). The lentiviral vector encoded a chimeric antigen receptor (CAR19) under the control of an internal human PGK promoter. The concentrated vector titre of this 'Terminal-TRAC' configuration (TT-hPGK-CAR19) was comparable to a conventional pCCL-hPGK-CAR19 vector ($1.6x10^8$/ml v $1.5x10^8$/ml) indicating that inclusion of the sgRNA cassette in the 3' LTR was not detrimental to vector titre, and supported comparable transduction efficiencies in primary T cells. Unique primer pairs amplified both 3' and 5' LTR regions in these cells (Figure 2A) and yielded the expected 392bp 3' U5 reaction product from the pCCL-hPGK-CAR19 transduced cells compared to a larger 755bp product from the TT-hPGK-CAR19 transduced cells. A 742bp 5' PCR product indicated duplication of the U6 promoter-sgRNA-scaffold sequences in contrast to a 379bp conventional duplication product. Bands were extracted and sequences verified by Sanger sequencing. Furthermore, quantitative RT-PCR found that guide RNA expression peaked between 24 and 72 hours after lentiviral transduction and thereafter remained stable during manufacture (Figure 2B).

Transient Cas9 mRNA delivery by electroporation to Terminal-TRAC T cells

Previous lentiviral configurations have incorporated Cas9 expression cassettes, but this could promote immunogenicity and result in on-going scission effects, risking toxicity. Stabilized Cas9 mRNA (capped, polyadenylated, and uridine modified) was delivered by electroporation for transient effects in dividing T cells exposed to a single round of transduction with TT-hPGK-CAR19 vector. An interval of 3 days was found to be optimal for TRAC disruption (Figure 2C). Cas9 protein was detected by Western blot as a 160kDa protein band, with peak expression at 12 hours after mRNA electroporation and clearance by 72 hours (Figure 2D). Titration of Cas9 mRNA mediated disruption of TCR expression exhibited saturation above 25μg/ml (Figure 2E). Molecular signatures of non-homologous end joining (NHEJ) at the TRAC locus were confirmed by PCR sequencing across the target locus and TIDE analysis of the 772bp TRAC amplicon (Figure 2F). Crucially, almost all cells expressing CAR19 were found to have disrupted TCR expression, indicating CRISPR-Cas9 effects were coupled to transgene expression.

Scalability of Terminal-TRAC T cell production

A critical hurdle for CRISPR/Cas9 gene editing is scalability and compliance for therapeutic manufacturing. We adapted an automated T cell lentiviral transduction procedure using the CliniMacs Prodigy system to compare alongside conventional cultures in G-Rex flasks, and activated $1x10^8$ lymphocytes from a thawed leukapheresis harvest ahead of lentiviral transduction with TT-hPGK-CAR19 vector at MOI 5 in the closed system tubing set (Figure 3A and Figure S1). After a further 72 hours, cells were removed from the device and electroporated with Cas9 mRNA, after which the cells were returned to the CliniMACS Prodigy and culture overnight at 30°C. After 11 days, CAR19

expression was 62% in CD45+CD2+ cells and TCR knockout in CD45+CD2+CAR19+ cells was 77% (Figure 3B). Further processing by magnetic bead mediated depletion of residual TCRαβ cells yielded a highly purified population of TCR depleted cells (>99%), almost all (96.9%) of which were CAR19+ T cells with a vector copy number (VCN) of 1.69 (Figure 3B). Disruption of the TRAC locus at the genomic level was verified by TIDE PCR (Figure 3C), which revealed NHEJ events of around 80% with next generation sequencing (NGS) detecting 'on-target' cleavage effects in 92% of sequence reads. Overall, a final cell yield of $2.9x10^9$ TT-CAR19+TCR- T cells was produced, almost 30x the starting number, and sufficient to create therapeutic doses for over 20 average adult subjects.

Terminal TRAC-CAR19+TCR- T cells efficiently target CD19+ cells in vitro

The cytolytic potential of TT-CAR19+TCR- cells was assessed by *in vitro* cytotoxicity against ^{51}Cr loaded CD19+ or CD19- SupT1 target cells. When normalized for CAR19+ cells, both TT-CAR19+TCR- cells and CAR19+TCR+ T cells exhibited comparable specific lysis of CD19+ Supt1 targets after 4 hours of co-culture, in contrast to non-transduced CAR19-TCR+ control cells ($P<0.0001$) (Figure 3D). Specific lysis of another CD19+ tumor line, Daudi, was also documented for CAR19+TCR+ and TT-CAR19+TCR- effectors and a 4-hour degranulation assay on this target cell line further corroborated the cytotoxicity data with 57% of CAR19+TCR- and 53% of CAR19+TCR+ cells upregulating CD107a expression (Figure 3E). Finally, a CBA assay recorded slightly increased cytokine production of IFNγ, TNF, IL-4 and IL-2 after 24 hours of co-culture with CD19+ Supt1 cells but not from CD19-Supt1 cells further confirming target specific effect (Figure 3F).

Characterisation of on- and off- target CRISPR effects.

Previously, we reported that T cells modified with a combination of TRAC and CD52 specific TALENs, exhibited translocation events involving the TRAC locus in around 4% of 500 interphase spreads using a dual-colour break-apart FISH probe for the TRAD locus (which incorporates the TRAC site)[4]. For TT-CAR19+ T cells, no breakpoints were identified within the sensitivity limits of the assay across 350 interphase spreads in Cas9 treated and across 600 interphase spreads in non-treated cells (Figure 4A). Further investigations compared these two populations using three independent modalities, based on WGS, targeted NGS and Digenome-seq. Predicted on-target Indel modifications captured by Digenome-seq had a score of 82.9%, corroborated by targeted amplification of the TRAC locus and analysis of >35,000 reads by NGS which revealed an Indel frequency of 92.3% versus 0.00% in non-edited cells (Figure 4B-C, Table S1 and Figure S2). In comparison, estimates by TIDE- PCR and 30x WGS had yielded lower modification efficiencies of 79% and 54% respectively reflecting less informed analysis techniques and lower read depths. Comparing events at 49 *in silico* predicted off-target sites by WGS and NGS and across ten additional gene loci with 14q translocation phenomena known to be associated with T cell leukemias (TAL1, LCK, REL, MYC, NOTCH1, TLX1, THUMPD1, BCL11B, TCL1A, TCL1B), there was no notable differences between the modified and non-modified samples (Table S1). In addition, Digenome-seq captured a further 12 off-target sites, of which 8 were distinct not having been predicted *in silico*, with 3/12 showing DNA cleavage scores between 3.5%-16% (Figure 4C-D and Table S2). However, further NGS-based interrogation of these 12 sites in TT-CAR19+TCR- DNA did not detect genomic disruption (Figure 4D and Table S2). Wider, unbiased genomic variant calling using read frequency-based significance

thresholding on WGS data, identified a comparable number of SNVs, insertions and deletions in both Cas9 treated and non-treated cells (Figure 4E).

Further analysis of 'CRISPR-specific' mutations in the WGS data, which considered sequences proximal to PAM motifs, found 61% of Indels were unique to TT-CAR19+TCR- Cas9 treated samples compared to 39% of changes in non-treated cells (Figure 4F). Similarly, translocation frequency was comparable in both samples (Figure 4G), with 57% of structural unique variants detected in Cas9 treated cells and 42% in non-treated samples (Figure 4H). Additional filtering of these sites identified 16 Cas9 treated and 14 non-treated changes as precise changes. Interestingly, one unpredicted site appeared to have been the subject of unanticipated modification. Chr3:128630177-128630178, encoding *RPN1* was found to have a 15% frameshift associated Indel frequency (8/50 reads) compared to 0/33 control sample reads. This site was not identified by Digenome-seq analysis, and further interrogation of the *RPN1* locus by NGS discounted these Indels, highlighting the limitations of low depth sequencing and emphasizing the need for multifaceted investigations. Importantly, at the cellular level, T cell function was preserved and there was no evidence of overt toxicity in the edited TT-CAR19+TCR- product.

Terminal TRAC T cell anti-leukemic activity in vivo

A humanized murine model of leukemic clearance was used to assess *in vivo* function of engineered CAR19 T cells. NSG mice inoculated intravenously with $5x10^5$ CD19+EGFP+Luciferase+ Daudi cells were imaged after 3 days, and then in groups of 8 animals, injected with either TT-CAR19+TCR-, CAR19+TCR+ or untransduced CAR19-TCR+ effector cells. Serial bioluminescence imaging was performed on days 7, 10 and 14, and half of the animals were then tracked for a further 14-21 days (Figure 5A-B).

There was rapid clearance of tumor in groups receiving CAR19+ T cells with negligible signal by day 14, in contrast to mice receiving non-transduced T cells or PBS (***P<0.001) (Figure 5A). Interestingly, TT-CAR19+TCR- (n=8) mediated clearance by day 14 was superior compared to clearance in CAR19+TCR+ T cells injected mice (n=8) (*P<0.05) based on bioluminescence quantification (Figure 5C). Flow cytometric analysis was undertaken for GFP+ Daudi cells and CD45+CD2+ effector T cell populations harvested from bone marrow of TT-CAR19+TCR- (n=4/8), CAR19+TCR+ (n=5/8), CAR19-TCR+ (n=5/8) and PBS (n=3/3) injected mice. By day 14, less than 0.01% (0.009% ±0.006%) of total marrow harvested from long bones of TT-CAR19+TCR- and <0.007% ±0.002% of CAR19+TCR+ injected mice expressed GFP Daudi cells indicating a highly significant (>45-fold) reduction compared to the 0.416% ±0.301% (*P<0.05) and 0.336% ±0.246% tumor content detected in the marrow of CAR19-TCR+ and PBS control animals respectively (Figure 5E).

By day 28, the remaining control CAR19-TCR+ animals had exhibited a further 125-fold increase in tumor burden and the mice were culled, revealing a low T cell to tumor ratio on flow analysis, despite a significant expansion of CD45+CD2+ T cells in the final two weeks. The remaining treatment groups were monitored until day 34 (Figure 5A). Radiance increased in the CAR19+TCR+ group but not the TT-CAR19+TCR- group (Figure 5C) during this period with bioluminescence signal appearing to localize in the bone marrow. This finding was supported by flow cytometry data which showed GFP+ Daudi cells in marrow had increased six fold in the CAR19+TCR+ group (*P<0.05) (Figure 5D-E). Interestingly, on further analysis, we found evidence of antigen escape with clearly demarcated populations of CD20+ GFP+ Daudi cells that had lost CD19+ expression in all three animals (Figure 5F).

The TT-CAR19+TCR- group exhibited the highest levels of CAR19+ T cells at both 2 and 5 weeks and had the lowest tumor burden (Figure 5E) retaining the highest T cell:tumor ratio throughout. In contrast, median CAR19 percentage was 34.5% (32.3-53.6) in CAR19+TCR+ treated mice at 2 weeks and this rose to 92.9% (47.4-93.9) by 5 weeks consistent with notable expansion of transduced populations. The intensity of CAR19 expression on flow cytometry was higher in the TCR- animals than TCR+, but the difference was not-significant. Interestingly, the TCR+ mice exhibited high levels (84.5% (55.6-89.8)) of the exhaustion marker PD-1 on T cells compared to 15.1% (8.2-20.4) at two weeks (Figure 5G). This was also documented in non-transduced CAR19-TCR+ controls where PD1 levels of 48.6% (37.6-49.9) at 2 weeks and 83.5% (34.9-99.1) at 4 weeks had been observed in predominantly CD4+ but also CD8+ T cells. Of note, TT-CAR19+TCR- effectors had the least exhausted phenotype with the lowest levels of PD1 expression of 6.8% (5.51-13.1) and 24.8% (16.0-50.0) at both 2 and 5 week time points, respectively.

Discussion

There is accumulating evidence for the efficacy of T cells engineered to express chimeric antigen receptors (CARs) against leukemia antigens such as CD19 in the management of relapsed B cell malignancies.[1] As well as autologous T cells, HLA-matched allogeneic T cells from hematopoietic stem cell donors have been used and recently non-HLA matched 'universal' CAR-T cells have entered clinical phase assessments.[4] These cells were edited using TALENs to disrupt the TRAC locus to prevent GVHD and at the CD52 locus to confer resistance to the lymphodepleting antibody alemtuzumab. The modification

process employed a multiplex approach, delivering mRNA encoding two highly specific TALEN pairs by electroporation which conferred high frequency allele modification but was also associated with predicted and unpredicted translocation events of unknown significance. In the case of the TRAC locus, in most T cells allelic exclusion operates to ensure that only a single TCRαβ configuration is expressed, and therefore NHEJ mediated disruption of the active allele is theoretically sufficient to disrupt cell surface TCRαβ expression. Downstream processing using CliniMacs TCRαβ magnetic bead depletion ensures removal of residual $TCR\alpha\beta^{+}$ cells and readily yields highly purified (>99%) $TCR\alpha\beta^{-}$ T cells. However, shortcomings of current TALEN based approaches includes variable lentiviral transduction efficiencies between batches, and in the absence of an enrichment strategy to ensure all cells are $CAR19^{+}$, variations in total cell dosing required to achieve a particular CAR19 dose. In turn, the total T cell dose is a critical parameter that is determined, and limited by, the absolute number of residual TCRαβ cells that might be adoptively transferred as part of the total cell dose. Under existing approaches, $TCR\alpha\beta^{-}$ cells may be $CAR19^{+}$ or $CAR19^{-}$, but by coupling gene-editing effects to CAR19 expression, the TT-CAR19 configuration yields highly purified T cells that are $CAR19^{+}TCR\alpha\beta^{-}$. This system has a number of advantages:- 1. The incorporation of the CRISPR guide into the 3' LTR mitigates against interference effects and ensures intact transgene expression for highly efficient transduction and TRAC editing effects; 2. Coupling effects become fully manifest after the completion of downstream processing and depletion of residual TCRαβ cells, by which stage the product is highly homogeneous $CAR19^{+}TCR\alpha\beta^{-}$; 3 Transient delivery and expression of Cas9 (as stabilized, reduced immunogenicity Cas9 mRNA) provides time-limited DNA cleavage effects and reduces the risk of immunogenicity and using this approach, manufacture of a single Cas9 mRNA batch can service multiple terminal vector-CRISPR RNA guide combinations, reducing

costs and saving time associated with the manufacture of bespoke raw materials for different CRISPR/Cas9 targets; 4. The process is readily incorporated into an automated manufacturing platform facilitating early clinical application.

Investigations into on- and off target effects in TALEN edited T cells have previously reported translocations between TRAC and CD52 target sites of up to 1%, and we previously found around 4-5% of cells exhibited abnormal karyotypes with evidence of various TRAD translocations found on breakpoint FISH probe analysis.[4] Similar analysis in TRAC modified TT-CAR19+TCR- T cells did not detect any similar segregation of these FISH probes, although the sensitivity limitations of FISH means that translocations may have occurred below the limits of detection. We used three different platforms to confirm TRAC specific activity and absence of off-target effects. Whole genome sequencing found comparable very low frequencies of Indel events across the genome, including exonic sequences, for both Cas9 treated and non-treated cells. While there was increased detection of structural variants in the edited samples, interrogation of the highest ranking *in silico* predicted off-target sites found edited and non-edited samples to have a similar frequency of changes in both WGS and higher resolution NGS outputs. Similar findings were recorded across ten additional genes known to be sites of 14q translocations associated with T cell leukemia. There are a number of important caveats and limitations to the application of WGS for analysis of gene editing effects, including limited read depth. Digenome-seq has the capacity to detect low frequency events (0.1%-1%) and the specificity of the TRAC guide sequence was validated with negligible off-target effects that were further interrogated by NGS and also found to be absent in Cas9 treated cells. Nuclease mediated effects below this level however, are difficult to confirm given the sequencing error rates.[15, 16] A single unpredicted site in RPN1 was identified by WGS and could have represented an off-target site for our TRAC specific but this was

discounted upon further interrogation by NGS and by Digenome-seq. This highlights a potential limitation of relying on low depth sequencing platforms, and suggests that a multi-platform approach using tools such as Digenome-seq [17] GUIDE-seq [18] or Lentivirus capture [19] coupled with high resolution sequencing is paramount.

Finally, in vivo modeling revealed that TT-CAR19 T cells mediated highly effective leukemic eradication with less evidence of exhaustion compared to conventional TCR expressing CAR19 T cells. The latter was unexpected given that characterization of CAR19 transduced populations by flow cytometry, cytokine array profiles and functional studies in vitro had not detected any notable differences between TCR depleted CAR19 cells and conventional TCR+ CAR19 T cells. In human:murine chimeras bearing Daudi B cell leukemia tumor inoculations, animals dosed with TT-CAR19 T cells exhibited potent anti-leukemic effects without xenoreactive GVHD within the period of testing, and reduced upregulation of the exhaustion marker PD1 compared to control groups that had retained TCR expression. This is consistent with previous murine studies [20] and clinical trials of donor derived human CAR19 T cells where TCR mediated co-activation may drive exhaustion.[21]

Interestingly, flow characterization of Daudi cell surface marking in mice treated with CAR19+TCR+ T cells revealed a notable proportion had clearly lost CD19 expression at the time of culling, and this was not evident in tumor cells recovered from control CAR19-TCR+ treated mice. This phenomenon is reminiscent of clinical reports from patients who relapsed with CD19 negative leukemia after a period of remission following CAR19 therapy and we speculate that CD19 tumor populations acquired a survival advantage and expanded in the face of CAR19 immunity, although the absence of similar expansions in TT-CAR19+TCR- treated mice requires further investigation with larger numbers of animals.

One advantage of T cell engineering using integrating vector systems has been their apparent resistance to possible transformational events as a result of vector integration, and to date there have been no reports of human T cell insertional mutagenesis. Even in animals, vector mediated leukemiagenesis in T cells has rarely been encountered, and only in highly stressed artificial model systems.[22] Similar resilience may be anticipated following gene-editing, although loci such as the TRAC site have known translocation associations with T cell leukemia. We screened such sites by WGS, and all were found to be intact. In the absence of informative animal models, cautious deployment and careful patient monitoring will be essential to determine risks in early phase trials. Similarly, modeling in immunodeficient mice is not representative of clinical scenarios where lymphodepleting conditioning is required to overcome host mediated rejection of non-matched 'universal' T cells, but accumulating experience in clinical trails is helping to determine the intensity of such regimens.

The terminal vector configuration described here utilized *Streptococcus pyogenes* Cas9 but is readily adapted for other similar nucleases [15, 23-25], nickases [26], deactivated Cas systems [27, 28], or cytidine deamination linked enzymes [29]. The proof of concept configuration described here has been adapted further to include multiple guide cassettes for multiplex modifications, including simultaneous B_2m disruption to deplete MHC class I expression and PD-1 disruption to promote T cell invigoration. The platform could, with certain revisions, also be used for targeted CAR insertion into the TRAC locus as recently described using Adeno-Associated Virus.[30] However, the first planned therapeutic applications will be more straightforward and will exploit coupling of CAR19 and TCRαβ depletion, as a bridging strategy to transplantation. Thereafter, multiple applications are envisaged where *ex vivo* cell manipulation requiring vector mediated integration of

transgenes encoding receptors, selection markers or suicide genes need to be combined with therapeutic editing effects.

Materials and Methods

CRISPR-CAR vector system

A third generation SIN lentiviral vector described previously [31] expressing a CAR19 transgene was subjected to cloning incorporating a HIV-1 cPPT element and mutated WPRE for the expression of a CAR19 transgene under the control of a human phosphoglycerate kinase (PGK) promoter was subjected to site directed mutagenesis to remove BbsI, BsmbI and SapI restriction sites using a QuickChange Lightning Kit (210518, Agilent Technologies, Santa Clara, USA). U6 and H1 CRISPR guide cassettes were then cloned into the ΔU3 region of the 3'LTR using In-Fusion HD Cloning Plus (638909, Takara Bio Europe, Saint-Germain-en-Laye, France). BbsI restriction sites were then incorporated between the Pol III promoter and scaffold sequences to allow for efficient guide sequence substitution. GeneART synthesized CRISPR cassettes (ThermoFisher Scientific, Massachusetts, USA) based on the Zhang group *Streptococcus pyogenes* Cas9 scaffold sequence [10] were cloned into the ΔU3 region of the 3'LTR. Concentrated vector preparations were produced by transient transfection of 293T cells as previously described.[32, 33]

Primary human lymphocyte culture and modification

Peripheral blood mononuclear cells (PBMCs) were isolated by Ficoll-Paque density gradient and subsequently activated with TransACT reagent (130-109-104, Miltenyi Biotech, Surrey, UK). Lymphocytes were cultured in TexMACS medium (130-097-196, Miltenyi Biotech) with 3% human AB serum (GEM-100-512-HI, Seralabs, Brussels, Belgium) and 100U/ml Proleukin IL-2 (Novartis, Surrey, UK). PBMCs were transduced with lentiviral vector 24 hours post activation at a multiplicity of infection (MOI) of 5 and Cas9 mRNA electroporation performed 3 days later. Lymphocytes were cultured until day

11 post activation, and were then cryopreserved in 90% FCS and 10% dimethylsulfoxide (DMSO). Scaled experiments Scaled experiments ultilized a semi-automated platform as recently described.[34] Briefly, the T-cell transduction (TCT) program was adapted on the CliniMACS Prodigy using the Tubing Set TS520 (130-019-002, Miltenyi Biotec) and used cryopreserved leukapheresis harvests (Allcells, Alameda, USA) cultured in TexMACS GMP Medium (170-076-307, Miltenyi Biotec) supplemented with 3% human AB serum (Seralabs) and 20ng/ml MACS GMP Human Recombinant IL-2 (170-076-146, Miltenyi Biotec).[34] Cells were activated with TransAct T cell reagent (Miltenyi Biotech) and transduced 24 hours post activation at an MOI of 5 and electroporated with Cas9 mRNA on day 4.

Detection of non-homologous end joining (NHEJ) events

PCR amplicons of genomic DNA were sequenced and analyzed using TIDE protocols (https://tide.nki.nl/).[35] (Further details in supplemental methods).

FISH studies

Translocation events involving the TRAD locus were investigated using a dual-color, break-apart FISH probe (Cytocell TCRAD LPH 047-S; 14q11, red/green fusion) to interrogate interphase nuclei. A normal signal pattern comprises 2 fusion signals and TRAD rearrangements exhibit segregated single red/green markers.

***In vitro* Cytotoxicity**

Cytotoxic function of CAR19-TCR+, CAR19+TCR+ and TT-CAR19+TCR- T cells was assessed by co-culture with ^{51}Cr loaded CD19+ or CD19- SupT1 target cells at increasing

effector to target ratios (E:T in a 96 well format for 4 hours at 37°C). Release of ^{51}Cr was quantified using a microplate scintillation counter and specific cytotoxicity calculated.

Next Generation Sequencing

On-target and potential off-target sites were amplified and using Phusion polymerase (New England BioLabs), and the resulting PCR amplicons were amplified again using TruSeq HT Dual Index primers to make a library. Libraries were then subjected to paired-end sequencing using MiniSeq (Illumina).

Digenome-seq

To induce Cas9-mediated *in vitro* cleavage of genomic DNA, 100nM Cas9 protein and 300nM TRAC-targeting sgRNA were incubated with 10μg genomic DNA in a reaction buffer of 500μl (100mM NaCl, 50mM Tris-HCl, 10mM MgCl2, 100μg/ml BSA, pH 7.9) at 37°C for 8 hours. Digested DNA was incubated with 50μg/ml RNase A (Qiagen) at 37°C for 30 minutes to remove sgRNA, and purified again with a DNeasy Tissue Kit (Qiagen). Digested genomic DNA was fragmented with Covaris system (Life Technologies), and ligated with adapters to produce libraries, which were subjected to WGS using HiSeq X Ten Sequencer (Illumina) at Macrogen. Cas9-mediated *in vitro* cleavage of genomic DNA was performed and DNA cleavage scores were calculated using a scoring system described previously.[17, 36]

Whole Genome Sequencing

Genomic DNA was extracted from CAR19+TCR+ and TT-CAR19+TCR- cells, using the DNeasy Blood and Tissue Kit (QIAGEN). Approximately 1.5μg of Genomic DNA was analysed at Applied Biological Materials Inc. (Richmond, B.C., Canada), by 30x WGS

using the MiSeq platform. Overall alignment rates were >99.9% and correct pairing >>98.3%. GATK and DELLY were used to identify single nucleotide variance, indels and other structural differences. Targeted assessment of the TRAC locus and 49 predicted possible off-target sites was undertaken as well as screening of ten known gene sites where translocations of 14q have known leukemic associations.

***In vivo* anti-tumor activity**

NOD/SCID/$\gamma c^{-/-}$ (NSG) mice, were inoculated IV with $5x10^5$ CD19+ Daudi tumor cells by tail vein injection on day 0. The tumor cells had been stably transduced to express both enhanced green fluorescent protein (EGFP) and Luciferase. Tumor engraftment was confirmed by *in vivo* imaging of bioluminescence using an IVIS Lumina III *In Vivo* Imaging System (PerkinElmer, Massachusetts, USA, live image version 4.5.18147) on day 3. Animals were injected on day 4 with either PBS (n=3), $5x10^6$ untransduced CAR19-TCR+ T cells (n=8), $8x10^6$ CAR19+TCR+ T cells (n=8) or $5x10^6$ TT-CAR19+TCR- T cells (n=8). Analysis of tumor clearance was performed by serial bioluminescent imaging and processing of bone marrow for the monitoring of tumor progression vs clearance was carried out on days 7, 10, 14, 18, 21, 28, and 35. Bone marrow samples were processed by a red blood cell lysis followed by staining for flow cytometry. All animal studies were approved by the University College London Biological Services Ethical Review Committee and licensed under the Animals (Scientific Procedures) Act 1986 (Home Office, London, United Kingdom). (Further details in supplemental methods).

Statistics

A two-tailed Man-Whitney U test was used for non-parametric comparison of grouped data and values are presented as mean percentages of three or more samples with standard

error of the mean (SEM) or standard deviation (SD) or as a median with the 25th and 75th percentiles (50% central range) stated. Linear Regression was used for the comparison of serial measurements, taking each Y value as an individual point. All statistical analysis was performed using GraphPad Prism software version 5.01.

Disclosures

AD, NH, AA hold interests/are employees of Desktop genetics.
WQ holds interests unrelated to this project in Autolus Ltd and Orchard Therapeutics.
WQ receives unrelated research funding from Cellectis, Servier, Miltenyi, Bellicum.

Author contributions

C.G., R.P. and W.Q., designed the project and wrote the manuscript. C.G. and R.P. developed the vector and performed *in vitro* and *in vivo* experiments and data analysis. L.N. managed the scale-up manufacture and assisted with the CBA assay. A.E. performed the degranulation assay. A.P. carried out analysis of on- and off-target sites by NGS. D.L. carried out FISH analysis. A.D, N.H-K. and A.A. undertook the WGS analysis for the characterization of predicted of on- and off-target effects. D.K. and J.S.K. performed off-target analysis by NGS, WGS and Digenome-seq.

Acknowledgments

Supported by National Institute of health research (NIHR) and Great Ormond Street Biomedical research centre, (BRC) and Children with Cancer. The views expressed are those of the author(s) and not necessarily those of the NHS, the NIHR or the Department of Health. We would like to extend our gratitude to Dr. Carolina Ferreira for her assistance and expertise in RT-PCR and WB assays.

References

1. Riviere, I, and Sadelain, M (2017). Chimeric Antigen Receptors: A Cell and Gene Therapy Perspective. *Mol Ther*.
2. Torikai, H, Reik, A, Liu, PQ, Zhou, Y, Zhang, L, Maiti, S, *et al.* (2012). A foundation for universal T-cell based immunotherapy: T cells engineered to express a CD19-specific chimeric-antigen-receptor and eliminate expression of endogenous TCR. *Blood* **119**: 5697-5705.
3. Provasi, E, Genovese, P, Lombardo, A, Magnani, Z, Liu, PQ, Reik, A, *et al.* (2012). Editing T cell specificity towards leukemia by zinc finger nucleases and lentiviral gene transfer. *NatMed* **18**: 807-815.
4. Qasim, W, Zhan, H, Samarasinghe, S, Adams, S, Amrolia, P, Stafford, S, *et al.* (2017). Molecular remission of infant B-ALL after infusion of universal TALEN gene-edited CAR T cells. *Science translational medicine* **9**.
5. Poirot, L, Philip, B, Schiffer-Mannioui, C, Le Clerre, D, Chion-Sotinel, I, Derniame, S, *et al.* (2015). Multiplex Genome-Edited T-cell Manufacturing Platform for "Off-the-Shelf" Adoptive T-cell Immunotherapies. *Cancer research* **75**: 3853-3864.
6. Bertaina, A, Merli, P, Rutella, S, Pagliara, D, Bernardo, ME, Masetti, R, *et al.* (2014). HLA-haploidentical stem cell transplantation after removal of alphabeta+ T and B cells in children with nonmalignant disorders. *Blood* **124**: 822-826.
7. Osborn, MJ, Webber, BR, Knipping, F, Lonetree, CL, Tennis, N, DeFeo, AP, *et al.* (2016). Evaluation of TCR Gene Editing Achieved by TALENs, CRISPR/Cas9, and megaTAL Nucleases. *Mol Ther* **24**: 570-581.
8. Ren, J, Zhang, X, Liu, X, Fang, C, Jiang, S, June, CH, *et al.* (2017). A versatile system for rapid multiplex genome-edited CAR T cell generation. *Oncotarget*.
9. Ren, J, Liu, X, Fang, C, Jiang, S, June, CH, and Zhao, Y (2016). Multiplex Genome Editing to Generate Universal CAR T Cells Resistant to PD1 Inhibition. *Clinical cancer research : an official journal of the American Association for Cancer Research*.
10. Shalem, O, Sanjana, NE, Hartenian, E, Shi, X, Scott, DA, Mikkelsen, TS, *et al.* (2014). Genome-scale CRISPR-Cas9 knockout screening in human cells. *Science* **343**: 84-87.
11. Adam, MA, Osborne, WR, and Miller, AD (1995). R-region cDNA inserts in retroviral vectors are compatible with virus replication and high-level protein synthesis from the insert. *Hum Gene Ther* **6**: 1169-1176.
12. Szulc, J, Wiznerowicz, M, Sauvain, MO, Trono, D, and Aebischer, P (2006). A versatile tool for conditional gene expression and knockdown. *NatMethods* **3**: 109-116.
13. Curtin, JA, Dane, AP, Swanson, A, Alexander, IE, and Ginn, SL (2008). Bidirectional promoter interference between two widely used internal heterologous promoters in a late-generation lentiviral construct. *Gene therapy* **15**: 384-390.
14. Hsu, PD, Lander, ES, and Zhang, F (2014). Development and applications of CRISPR-Cas9 for genome engineering. *Cell* **157**: 1262-1278.
15. Kleinstiver, BP, Pattanayak, V, Prew, MS, Tsai, SQ, Nguyen, NT, Zheng, Z, *et al.* (2016). High-fidelity CRISPR-Cas9 nucleases with no detectable genome-wide off-target effects. *Nature* **529**: 490-495.

16. Tycko, J, Myer, VE, and Hsu, PD (2016). Methods for Optimizing CRISPR-Cas9 Genome Editing Specificity. *Mol Cell* **63**: 355-370.
17. Kim, D, Bae, S, Park, J, Kim, E, Kim, S, Yu, HR, *et al.* (2015). Digenome-seq: genome-wide profiling of CRISPR-Cas9 off-target effects in human cells. *Nature methods* **12**: 237-243, 231 p following 243.
18. Tsai, SQ, Zheng, Z, Nguyen, NT, Liebers, M, Topkar, VV, Thapar, V, *et al.* (2015). GUIDE-seq enables genome-wide profiling of off-target cleavage by CRISPR-Cas nucleases. *Nature biotechnology* **33**: 187-197.
19. Knipping, F, Osborn, MJ, Petri, K, Tolar, J, Glimm, H, von Kalle, C, *et al.* (2017). Genome-wide Specificity of Highly Efficient TALENs and CRISPR/Cas9 for T Cell Receptor Modification. *Molecular therapy Methods & clinical development* **4**: 213-224.
20. Jacoby, E, Yang, Y, Qin, H, Chien, CD, Kochenderfer, JN, and Fry, TJ (2016). Murine allogeneic CD19 CAR T cells harbor potent antileukemic activity but have the potential to mediate lethal GVHD. *Blood* **127**: 1361-1370.
21. Ghosh, A, Smith, M, James, SE, Davila, ML, Velardi, E, Argyropoulos, KV, *et al.* (2017). Donor CD19 CAR T cells exert potent graft-versus-lymphoma activity with diminished graft-versus-host activity. *Nat Med* **23**: 242-249.
22. Newrzela, S, Cornils, K, Li, Z, Baum, C, Brugman, MH, Hartmann, M, *et al.* (2008). Resistance of mature T cells to oncogene transformation. *Blood* **112**: 2278-2286.
23. Ran, FA, Cong, L, Yan, WX, Scott, DA, Gootenberg, JS, Kriz, AJ, *et al.* (2015). In vivo genome editing using Staphylococcus aureus Cas9. *Nature* **520**: 186-191.
24. Zetsche, B, Gootenberg, JS, Abudayyeh, OO, Slaymaker, IM, Makarova, KS, Essletzbichler, P, *et al.* (2015). Cpf1 is a single RNA-guided endonuclease of a class 2 CRISPR-Cas system. *Cell* **163**: 759-771.
25. Fonfara, I, Richter, H, Bratovic, M, Le Rhun, A, and Charpentier, E (2016). The CRISPR-associated DNA-cleaving enzyme Cpf1 also processes precursor CRISPR RNA. *Nature* **532**: 517-521.
26. Ran, FA, Hsu, PD, Lin, CY, Gootenberg, JS, Konermann, S, Trevino, AE, *et al.* (2013). Double nicking by RNA-guided CRISPR Cas9 for enhanced genome editing specificity. *Cell* **154**: 1380-1389.
27. Maeder, ML, Linder, SJ, Cascio, VM, Fu, Y, Ho, QH, and Joung, JK (2013). CRISPR RNA-guided activation of endogenous human genes. *Nature methods* **10**: 977-979.
28. Perez-Pinera, P, Kocak, DD, Vockley, CM, Adler, AF, Kabadi, AM, Polstein, LR, *et al.* (2013). RNA-guided gene activation by CRISPR-Cas9-based transcription factors. *Nature methods* **10**: 973-976.
29. Komor, AC, Kim, YB, Packer, MS, Zuris, JA, and Liu, DR (2016). Programmable editing of a target base in genomic DNA without double-stranded DNA cleavage. *Nature* **533**: 420-424.
30. Eyquem, J, Mansilla-Soto, J, Giavridis, T, van der Stegen, SJ, Hamieh, M, Cunanan, KM, *et al.* (2017). Targeting a CAR to the TRAC locus with CRISPR/Cas9 enhances tumour rejection. *Nature* **543**: 113-117.
31. Dull, T, Zufferey, R, Kelly, M, Mandel, RJ, Nguyen, M, Trono, D, *et al.* (1998). A third-generation lentivirus vector with a conditional packaging system. *The Journal of Virology* **72**: 8463-8471.
32. Demaison, C, Parsley, K, Brouns, G, Scherr, M, Battmer, K, Kinnon, C, *et al.* (2002). High-level transduction and gene expression in hematopoietic repopulating cells using a human immunodeficiency [correction of

imunodeficiency] virus type 1-based lentiviral vector containing an internal spleen focus forming virus promoter. *HumGene Ther* **13**: 803-813.

33. Qasim, W, Mackey, T, Sinclair, J, Chatziandreou, I, Kinnon, C, Thrasher, AJ, *et al.* (2007). Lentiviral vectors for T-cell suicide gene therapy: preservation of T-cell effector function after cytokine-mediated transduction. *MolTher* **15**: 355-360.
34. Mock, U, Nickolay, L, Philip, B, Cheung, GW, Zhan, H, Johnston, IC, *et al.* (2016). Automated manufacturing of chimeric antigen receptor T cells for adoptive immunotherapy using CliniMACS prodigy. *Cytotherapy* **18**: 1002-1011.
35. Brinkman, EK, Chen, T, Amendola, M, and van Steensel, B (2014). Easy quantitative assessment of genome editing by sequence trace decomposition. *Nucleic acids research* **42**: e168.
36. Kim, D, Kim, S, Kim, S, Park, J, and Kim, JS (2016). Genome-wide target specificities of CRISPR-Cas9 nucleases revealed by multiplex Digenome-seq. *Genome research* **26**: 406-415.

Figure legends

Figure 1. Terminal CRIPSR-CAR coupled lentiviral vector configuration. (A) Schema of CAR 19 expression for the targeted killing of CD19+ B cells, with simultaneous CRISPR mediated TCR disruption, where ideally all T cells are CAR19+ and TCR- **(B)** Self inactivating lentiviral plasmid configuration coupling terminal TRAC (TT) CRISPR guide RNA and CAR19 transgene expression. A human PolIII promoter-sgRNA CRISPR cited in the deleted unique (ΔU3) region, proximal to repeat (R) elements of the 3'long terminal repeat (LTR). **(C)** Following reverse transcription, 3' LTR elements, including the PolIII-sgRNA cassette, duplicate to the 5'LTR of the proviral vector. **(D)** single-guide RNA (sgRNA) expressed from both 5' and 3' LTR vector elements forms ribonucleoprotein complexes with Cas9 following electroporation of Cas9 mRNA, and this effect is restricted to transduced populations.

CMV, Cytomegalovirus promoter; LTR: long terminal repeat; hPGK: human phosphoglycerate kinase promoter; cPPT: central polypurine tract; WPRE: woodchuck post transcriptional-regulatory element; gRNA: guide-RNA; sgRNA: single-guide RNA; vH/vL: variable heavy or light chain; TCR: T cell receptor

Figure 2. Validation of Terminal CRISPR-CAR vector and titration of Cas9-mediated knockout effect in primary human T cells. (A) PCR amplification of proviral 5' LTR elements, spanning the ΔU3 and Psi regions (755bp band) and 3'LTR (742bp band) confirmed the presence of duplicated PolIII-sgRNA in T cells transduced with TT-CAR19. **(B)** RT-qPCR measurement of TRAC sgRNA fold change at 0, 1, 3, 4, 7 and 11 days post transduction shows stabilization of sgRNA expression after 4 days. **(C)** Quantification of TCR knockout following Cas9 mRNA electroporation of primary T cells at 1, 2, 3, 4, 7 or 11 days post TT-CAR19 transduction showing optimal TCR disruption occurring at 3-4 day time point. Percent knockout calculated by flow cytometry based detection of TCR expression in CAR19+ population. **(D)** Following Cas9 mRNA electroporation, Cas9 protein expression detected as a 160 kda band peaked after 12 hours and became undetectable by 72 hours. β-actin detection (42 kda) verified protein loading. **(E)** Coupling of transgene expression and TCR disruption effects across a gradient of Cas9 mRNA concentrations in TT-CAR19 transduced PBMCs exhibiting >70% CAR19 expression. **(F)** PCR amplification and analysis by TIDE algorithm for the detection of NHEJ signatures across the TRAC locus confirmed Cas9 dose dependent scission and repair effects.

Figure 3. Scalability and *in vitro* functional integrity of TT-CAR19+TCR- T cells. **(A)** Scaled manufacture of homogenous TT-CAR19+TCR- cells using a semi-automated process on a CliniMACS Prodigy device in combination with off-device electroporation. Control cultures were separated and cultured in G-Rex 10 flasks at relevant stages. Following anti-CD3/anti CD28 activation, lentiviral, transduction and Cas9 mRNA electroporation, T cells were expanded in the integrated cultivation chamber before magnetic bead depletion of residual TCRαβ cells. As a consequence, coupled TCR knockout effects and CAR expression was assured in the final product. **(B)** Flow cytometry of untransduced (UTD) and cells transduced with TT-CAR19 but not supplied with Cas9 provided comparator data. Addition of Cas9 mRNA by electroporation resulted TCR loss in >52% of cells, and this population was enriched to >99% by TCRαβ depletion using magnetic beads. The resulting population was >97%CAR19+. **(C)** PCR amplification and analysis by TIDE algorithm of the TRAC locus in TT-CAR19 T cells with and without Cas9 mRNA electroporation confirming on-target NHEJ repair signatures. **(D)** Comparable CD19 specific cytotoxicity against ^{51}Cr labelled CD19+ SupT1 cells across a range of CAR19+ Effector:Target ratios was detected for CAR19+TCR+ (green) and TT-CAR19+TCR- effectors (red) (P=0.4461) but not for UTD CAR19-TCR+ populations (blue) (P<0.0001), indicating intact effector function after the additional processing steps required to generate universal cells. CD19- control targets confirmed specificity (dotted lines) P< 0.0001. Error bars represent standard error of the mean (n=3). Linear regression analysis showed significance between CAR19-TCR+ and CAR19+TCR+ (F=70.37, DFn=1, DFd=36, P<0.0001) or TT-CAR19+TCR- (F=47.65, DFn=1, DFd=44, P<0.0001) effectors against CD19+ Supt1 targets. No significance seen between CAR19+TCR+ and TT-CAR19+TCR- effectors (F=0.59, DFn=1, DFd=36, P=0.45). **(E)** CD107a degranulation responses detected by flow

cytometry were also comparable in CAR19+TCR+ and TT-CAR19+TCR- effectors when co-cultured with CD19+ Daudi targets. PMA and ionomycin stimulation of TT-CAR19+TCR- effectors served as positive controls for the detection of HLA-DR, IFNγ, CD107a and CD25. Error bars represent SEM of technical replicates (n=3). **(F)** Flow cytometric detection of cytokines in supernatant from co-cultures with SupT1 targets found comparable levels of IFNγ and TNFα for CAR19+TCR+ and TT-CAR19+TCR- effectors. Error bars represent SEM of technical replicates (n=3).

Figure 4. Off-target analysis by FISH, Digenome-seq and WGS. (A) TRAD FISH probe (Cytocell) – red centromeric end - green telomeric end to the TCR gene. Two fusions (green/red) present showed no rearrangement of the TRAD locus in TT-CAR19+TCR-(+Cas9) treated samples. **(B)** Digenome-seq captured on-target cleavage of the TRAC locus, chr14. Straight alignment in TRAC sgRNA SpCas9 digested DNA indicated on-target cleavage of the TRAC locus compared to staggered alignment of untreated DNA. **(C)** On- and off-target capture by Digenome-seq in TRAC sgRNA SpCas9 treated DNA displaying on-target cleavage (chr14) and off-target events in chr7 and chr15. **(D)** Cleavage scores in 12 chromosomal locations captured by Digenome-seq as off-targets in TRAC sgRNA SpCas9 treated DNA. High-resolution NGS-based validation of captured off-target sites in TT-CAR19+TCR- DNA shows absence of off-target Indels. **(E)** Genomic variants (SNVs, deletions and insertions) identified by 30X WGS and classed as significant by frequency of detection showed comparable counts in both CAR19+TCR+(-Cas9) treated and TT-CAR19+TCR-(+Cas9) treated samples. **(F)** "CRISPR-specific" Indels identified to be unique to each sample exhibit higher frequency in edited TT-CAR19+TCR-(+Cas9) sample. **(G)** Comparative frequency of structural variant (translocations) counts considered to be significant (at least 2 supporting reads)

after 30X WGS analysis in CAR19+TCR+(-Cas9) treated and TT-CAR19+TCR-(+Cas9) samples. **(H)** Translocations unique to each sample as part of total reads (F) reveals minor increase in TT-CAR19+TCR-(+Cas9) treated sample.

Figure 5. Human:murine leukemia responses by TT-CAR19+ effector T cells against CD19+GFP/Luciferase Daudi targets. (A) Serial bioluminescence imaging (BLI) of NSG mice following intraperitoneal administration of D-luciferin substrate. **(B)** Timeline of tumor and effector cell injection, BLI and organ harvest time points over the 5wk period. **(C)** Progressive increases in radiance [p/s/cm^2/sr] in non-treated (n=3) or control CAR19-TCR+ (n=8) effector groups indicated leukemic progression within 2 weeks (wk) and resulted in death by 4wk of the three animals subjected to extended monitoring. Mice injected with CAR19+TCR+ (n=8) or TT-CAR19+TCR- (n=8) effectors exhibited significantly delayed leukemic progression by 2wk compared to CAR19-TCR+ (P=0.0002), as tracked for 5wks in in three animals with CAR19+TCR+ and four with TT-CAR19+TCR- cells. The latter exhibited the lowest disease radiance at termination P<0.0001, error bars represent SEM. Linear regression analysis showed significance amongst all groups: CAR19+TCR+ vs. CAR19-TCR+ (F=29.79, DFn=1, DFd=87, P<0.0001), TT-CAR19+TCR- vs. CAR19-TCR+ (F=53.77, DFn=1, DFd=92, P<0.0001), TT-CAR19+TCR- vs. CAR19+TCR+ (F=8.93577, DFn=1, DFd=95, P=0.0036). Dotted lines represent Mann-Whitney U test (*P=0.0499, ***P=0.0002). **(D)** Representative flow cytometry plots gated on human CD45+ populations in bone marrow (BM) demonstrating a greatly reduced, but well demarcated population of GFP+ leukemia in CAR19+TCR+ treated mice [n=5 (2wk)/n=3 (5wk)] compared to UTD CAR19-TCR+ cohort [n=5 (2wk)/n=3 (4wk)]. In contrast leukemia was barely detectable in TT-CAR19+TCR- treated animals [n=4 (2wk)/n=4 (5wk)]. Human T cells were detected as CD2+ cells in all groups. **(E)** Disease burden after 2wk and at termination in BM was highest in control CAR19-TCR+ (blue circles) treated animals [(n=5 (2wk)/n=3 (4wk)]. Disease was barely detected in TT-CAR19+TCR- (red triangles) animals [(n=4 (2wk)/n=4 (5wk)), and found to be significantly reduced compared to CAR19+TCR+ (green squares) effector group

[(n=5 (2wk)/n=3 (5wk)) at termination when compared to CAR19-TCR+ 2wk values (*P*=0.0357 vs. *P*=0.0159), error bars represent SEM. **(F)** Phenotypic assessment of leukemia in BM at termination uncovered the emergence of CD19-CD20+ Daudi populations in animals treated with CAR19+TCR+ cells (n=3), whereas the leukemia detected in control animals CAR19-TCR+ (n=3) was CD19+CD20 and the paucity of leukemia cells in TT-CAR19+TCR- animals (n=4) precluded further characterisation. **(G)** Representative flow cytometric data from CAR19-TCR+ [(n=5 (2wk)/n=3 (5wk)), CAR19+TCR+ [(n=5 (2wk)/n=3 (4wk)) or TT-CAR19+TCR- [(n=4 (2wk)/n=4 (5wk)) treated animals showing PD1 expression on T cells. Markedly increased expression in CAR19-TCR+ and CAR19+TCR+ T cell injected groups measured at 2wk and at termination compared to initial expression levels in cells measured in vitro (CAR19-TCR+: 20.4%; CAR19+TCR+: 20.5%; TT-CAR19+TCR-: 9.7%) before infusion into mice. CAR19+TCR+ cells showed the highest increase in PD1 at termination over CAR19-TCR+ and TT-CAR19+TCR- groups.

eTOC Synopsis for MTJ-17-1909R1:

Long Terminal Repeat CRISPR-CAR coupled 'universal' T cells mediate potent anti-leukemic effects

Christos Georgiadis[1*], Roland Preece[1*], Lauren Nickolay[1], Aniekan Etuk[1], Anastasia Petrova[1], Dariusz Ladon[2], Alexandra Danyi[3], Neil Humphryes-Kirilov[3], Ayokunmi Ajetunmobi[3], Daesik Kim[4], Jin-Soo Kim[4], Waseem Qasim[1,2]

Georgiadis *et al.* combine a lentiviral chimeric antigen receptor (CAR) vector with CRISPR guides incorporated into the 3'LTR with transient Cas9 mRNA delivery for coupled gene modification effects. Processing through an automated platform to remove residual TCRαβ-cells was scalable and yielded highly enriched 'universal' T-cells, with potent anti-leukemic effects.

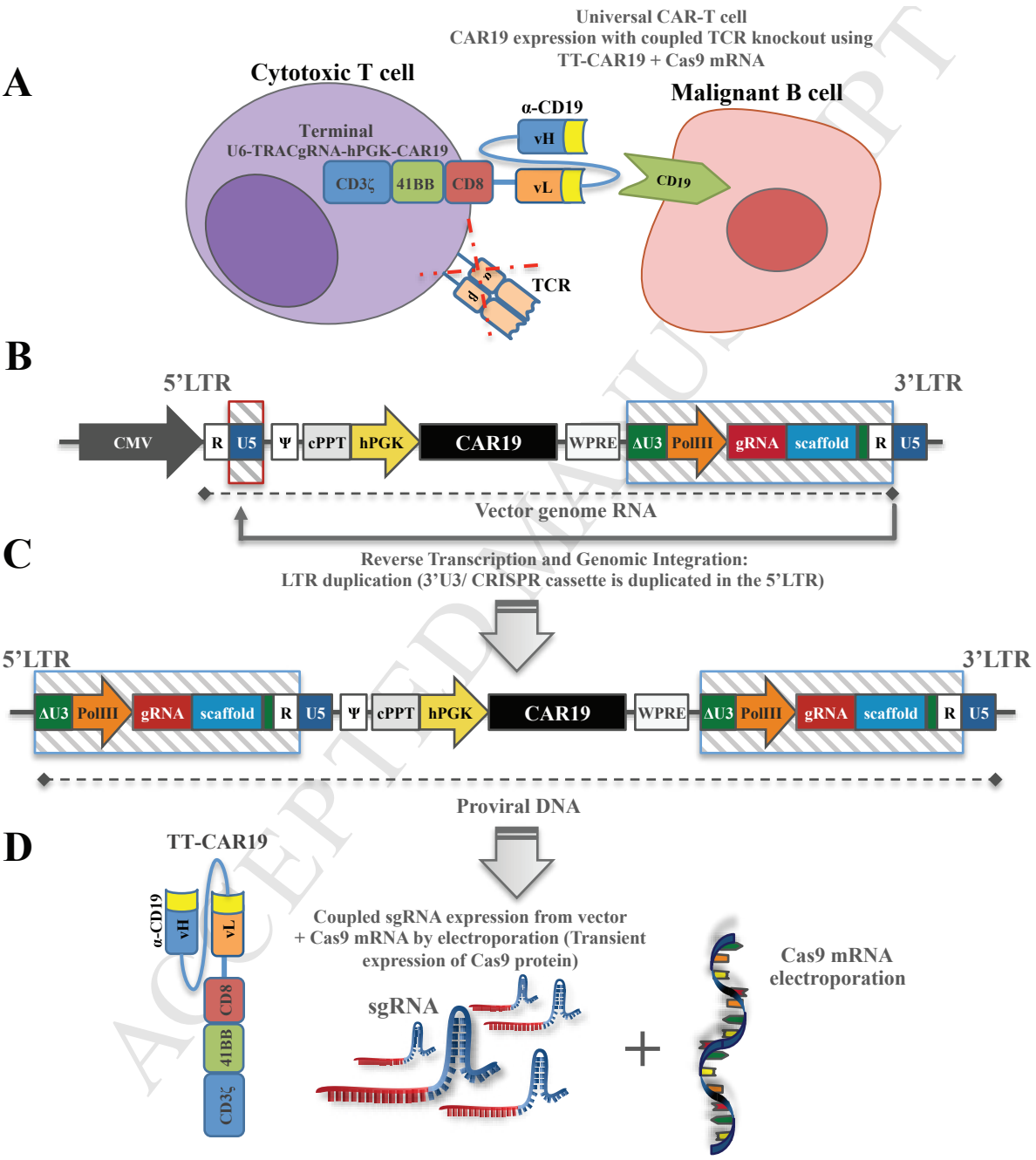
A
Universal CAR-T cell
CAR19 expression with coupled TCR knockout using
TT-CAR19 + Cas9 mRNA
Cytotoxic T cell
Terminal
U6-TRACgRNA-hPGK-CAR19
CD3ζ
41BB
CD8
α-CD19
vH
vL
Malignant B cell
CD19
TCR
B
5'LTR
3'LTR
CMV
R
U5
Ψ
cPPT
hPGK
CAR19
WPRE
ΔU3
PolIII
gRNA
scaffold
Vector genome RNA
C
Reverse Transcription and Genomic Integration:
LTR duplication (3'U3/ CRISPR cassette is duplicated in the 5'LTR)
Proviral DNA
D
TT-CAR19
Coupled sgRNA expression from vector
+ Cas9 mRNA by electroporation (Transient
expression of Cas9 protein)
sgRNA
Cas9 mRNA
electroporation

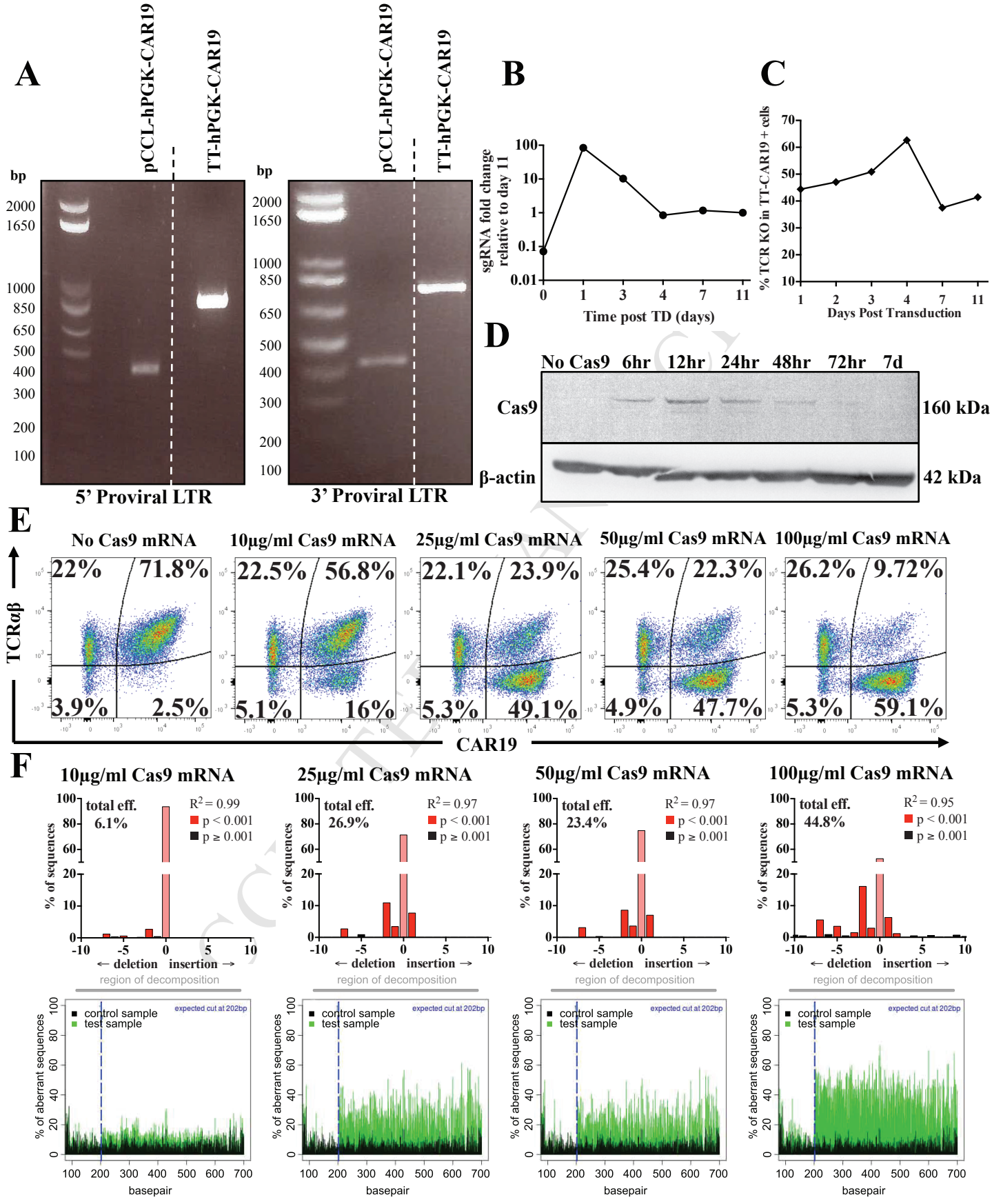
A
pCCL-hPGK-CAR19
TT-hPGK-CAR19
bp
2000
1650
1000
850
650
500
400
300
200
100
5' Proviral LTR
3' Proviral LTR
B
sgRNA fold change relative to day 11
Time post TD (days)
C
% TCR KO in TT-CAR19 + cells
Days Post Transduction
D
No Cas9 6hr 12hr 24hr 48hr 72hr 7d
Cas9
β-actin
160 kDa
42 kDa
E
No Cas9 mRNA
10µg/ml Cas9 mRNA
25µg/ml Cas9 mRNA
50µg/ml Cas9 mRNA
100µg/ml Cas9 mRNA
TCRαβ
CAR19
22% 71.8% 3.9% 2.5%
22.5% 56.8% 5.1% 16%
22.1% 23.9% 5.3% 49.1%
25.4% 22.3% 4.9% 47.7%
26.2% 9.72% 5.3% 59.1%
F
10µg/ml Cas9 mRNA
25µg/ml Cas9 mRNA
50µg/ml Cas9 mRNA
100µg/ml Cas9 mRNA
total eff. 6.1%
total eff. 26.9%
total eff. 23.4%
total eff. 44.8%
R2 = 0.99
R2 = 0.97
R2 = 0.97
R2 = 0.95
p < 0.001
p ≥ 0.001
% of sequences
← deletion insertion →
region of decomposition
control sample
test sample
expected cut at 202bp
% of aberrant sequences
basepair

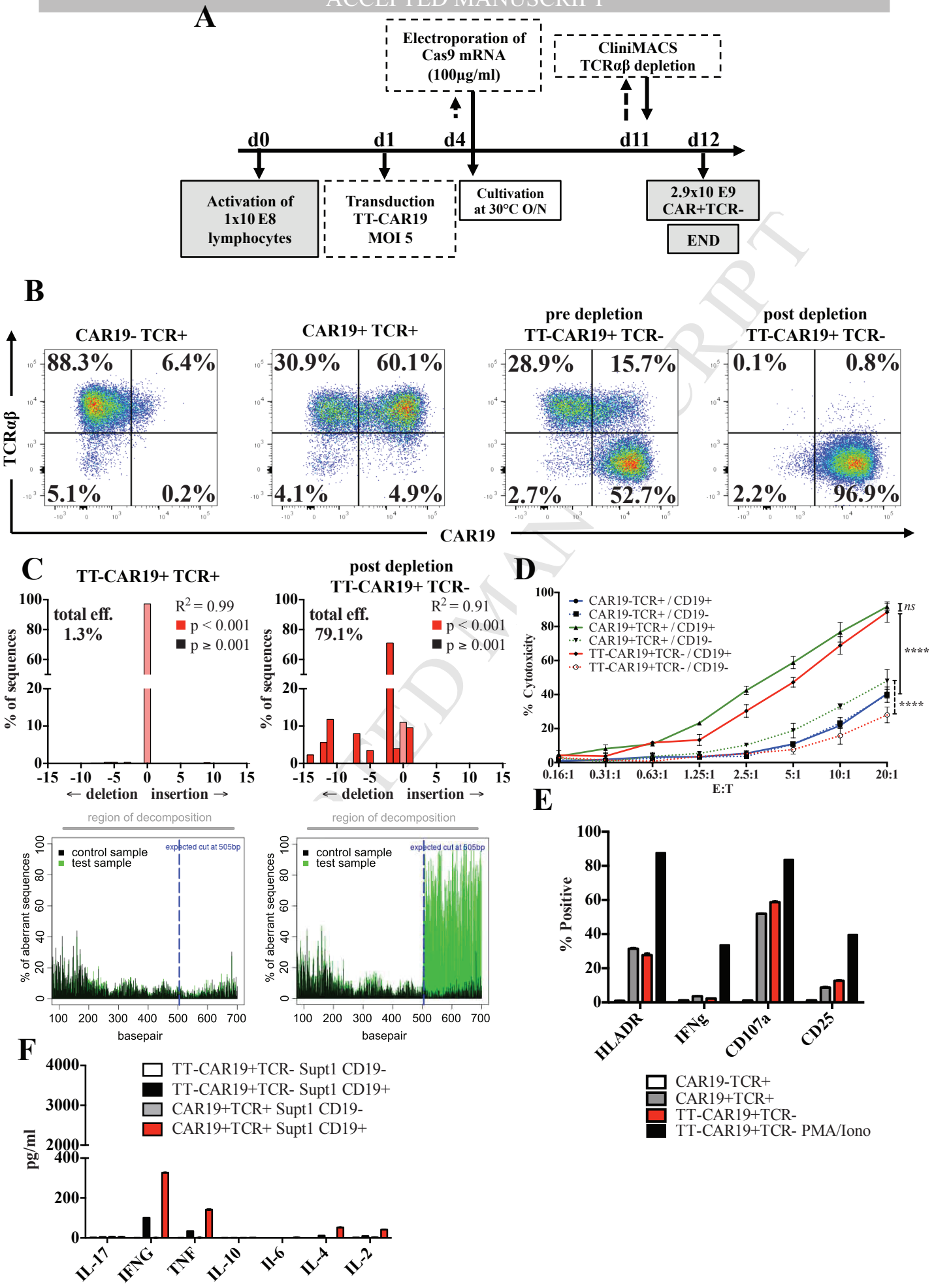

A

TT-CAR19+ TCR-

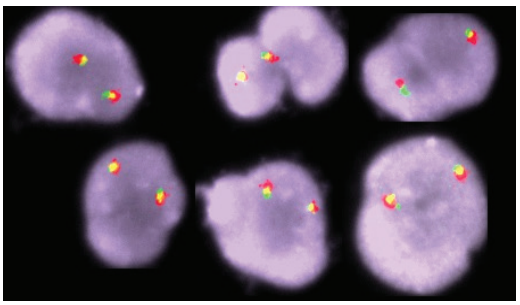

TCRAD FISH probe
centromeric end (red) /
telomeric end (green) of TCR gene

B

staggered alignment

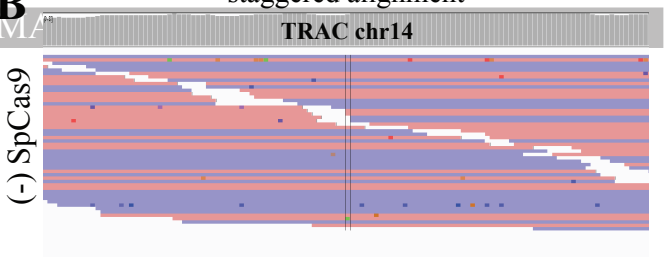

straight alignment

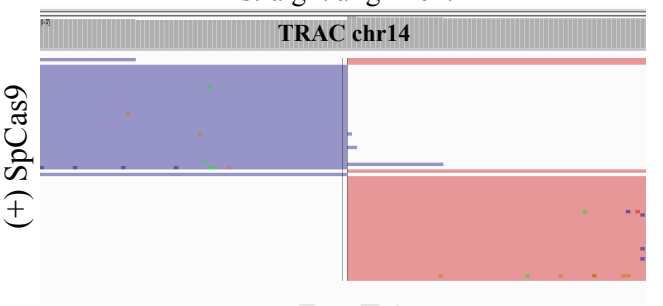

C

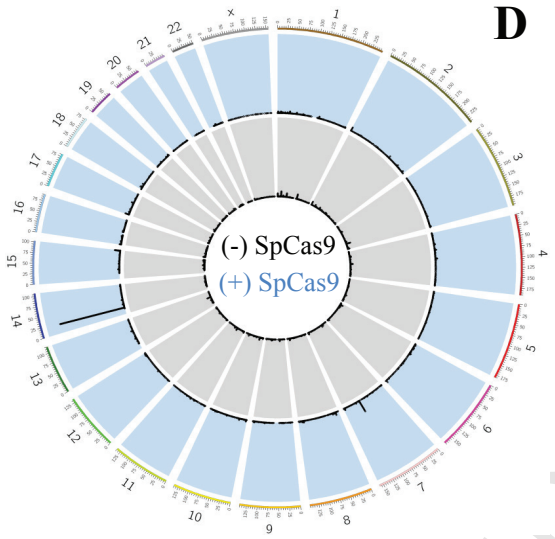

D

	Chr	DNA sequence at cleavage site	Digenome-seq DNA cleavage score	TT-CAR19+TCR- NGS Indel frequency (%)
TRAC	chr14	TCTCTCAGCTGGTACACGGCAGG	82.9	92.37
OT1	chr7	TCTCagAGCTGGTACACaGCAGG	15.5	0.01
OT2	chr15	TCTCatAGCTGGTACAtGGCGGG	6.9	0.02
OT3	chr8	TCTCaCAGCTGGaACACaGCAGG	3.6	0.00
OT4	chr1	cCcCTCAGCaGGTACACaGCCGG	1.9	0.00
OT5	chr1	agcCagAGCTGGTACACGGCTGG	1.9	0.01
OT6	chr7	ctgCTCAGCTGGTACACaGaAGG	1.3	0.01
OT7	chr1	gCTCTCAcCTGGTACACaGtGGG	0.7	0.00
OT8	chr12	ggaCTCAGaTGGcACACGGCAGG	0.5	0.01
OT9	chr1	TtTCTCAGCTGGTACAtGGaGGG	0.4	0.02
OT10	chr10	cCTCTCAGaTGGcACACGaCTGG	0.2	0.01
OT11	chr16	gggCaCAGCTGGTACACaGCAGG	0.1	0.00
OT12	chr11	gCTCTCAGCaGGTACACGGtCCAG	0.1	0.05

E

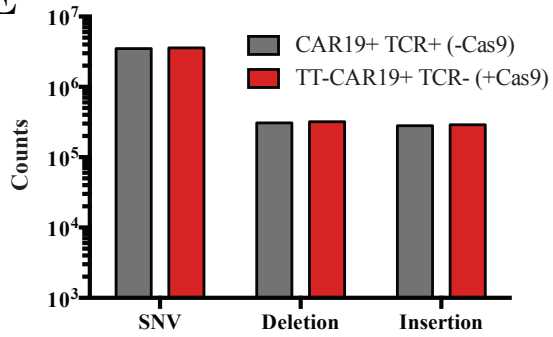

F

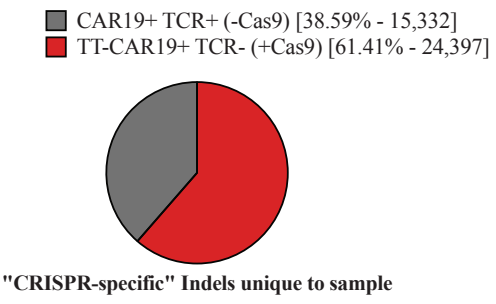

G

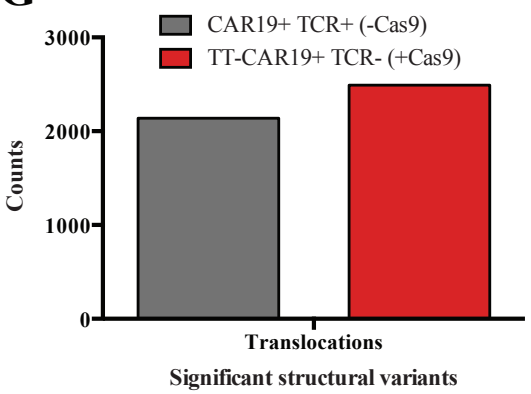

H